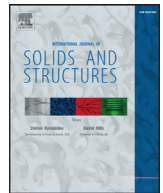




Contents lists available at ScienceDirect

International Journal of Solids and Structures

journal homepage: www.elsevier.com/locate/ijsolstr

Fading regularization MFS algorithm for inverse boundary value problems in two-dimensional linear elasticity

Liviu Marin^{a,b,*}, Franck Delvare^{c,d,e}, Alain Cimetière^f^a Department of Mathematics, Faculty of Mathematics and Computer Science, University of Bucharest, 14 Academiei, 010014 Bucharest, Romania^b Institute of Solid Mechanics, Romanian Academy, 15 Constantin Mille, 010141 Bucharest, Romania^c Normandie Univ, France^d UNICAEN, LMNO, F-14032 Caen, France^e CNRS, UMR 6139, F-14032 Caen, France^f Institute Pprime, CNRS-ENSMA-University of Poitiers, UPR 3346, Boulevard Marie et Pierre Curie, BP 30179 F-86962 Chasseneuil Futuroscope Cedex, France

ARTICLE INFO

Article history:

Received 5 May 2015

Revised 15 July 2015

Available online xxx

Keywords:

Linear elasticity

Inverse boundary value problem

Cauchy problem

Regularization

Method of fundamental solutions (MFS)

Iterative method

ABSTRACT

We investigate the numerical reconstruction of the missing displacements (Dirichlet data) and tractions (Neumann data) on an inaccessible part of the boundary in the case of two-dimensional linear isotropic elastic materials from the knowledge of over-prescribed noisy measurements taken on the remaining accessible boundary part. This inverse problem is solved using the fading regularization method, originally proposed by Cimetière et al. (2000, 2001) for the Laplace equation, in conjunction with a meshless method, namely the method of fundamental solutions (MFS). The stabilisation of the numerical method proposed herein is achieved by stopping the iterative procedure according to Morozov's discrepancy principle (Morozov, 1966).

© 2015 Elsevier Ltd. All rights reserved.

1. Introduction

Numerous boundary value problems in elasticity are characterised by incomplete boundary conditions. More precisely, for these inverse problems, both the traction and the displacement vectors are unknown and have to be determined on a part of the boundary of the solution domain occupied by the elastic solid. It is well-known that such inverse problems are in general ill-posed, in the sense that the existence, uniqueness and stability of their solutions are not always guaranteed, (see e.g. Hadamard, 1923). The lack of complete boundary conditions, encountered in the case of inverse boundary value problems, is usually overcome by supplying additional information in the form of either internal displacement, strain or stress measurements, or over-specified boundary conditions on the aforementioned accessible boundary. There are numerous important contributions in the literature, as well as various approaches, devoted to theoretical and numerical solutions of inverse boundary value problems in elasticity. For an extensive overview of inverse problems in elasticity over

the last decades, we refer the reader to Bonnet and Constantinescu (2005).

In general, there are two major classes of regularization methods used for the stable solution of inverse boundary value problems in linear elasticity, namely non-iterative/direct and iterative methods, respectively. The first class is usually based on either the minimization of a Tikhonov functional (or, equivalently, the resolution of the normal equation) (Tikhonov and Arsenin, 1986) or the decomposition of the matrix corresponding to the discretised system of equations, e.g. using the singular value decomposition (SVD) (Hansen, 1998), which is successively used to solve a sequence of well-conditioned problems depending on the regularization parameter. Finally, the value of the regularization parameter and, consequently, the corresponding regularized solution, are selected using an appropriate criterion, such as the discrepancy principle (Morozov, 1966), the generalized cross-validation criterion (Golub et al., 1979) or the L-curve method (Hansen, 1998). For inverse boundary value problems in elasticity tackled in this manner, we refer the reader to Schnur and Zabarar (1990), Gao and Mura (1991), Martin et al. (1995), Turco (1999), Marin and Lesnic (2002a), Marin and Lesnic (2002b), Marin and Lesnic (2004), Marin (2005), etc.

With respect to the second class of regularization methods used for inverse boundary value problems in elasticity, namely the so-called iterative regularizing methods, it should be mentioned that the Cauchy problem in elasticity was studied theoretically by

* Corresponding author at: Department of Mathematics, Faculty of Mathematics and Computer Science, University of Bucharest, 14 Academiei, 010014 Bucharest, Romania. Tel. +40 21 3126736.

E-mail addresses: marin.liviu@gmail.com, liviu.marin@fmi.unibuc.ro (L. Marin), franck.delvare@unicaen.fr (F. Delvare), alain.cimetiere@univ-poitiers.fr (A. Cimetière).

Yeih et al. (1993), who analysed its existence, uniqueness and continuous dependence on the data and proposed the fictitious boundary indirect method based on simple and double layer potential theory. The numerical implementation of this method was undertaken by Koya et al. (1993), who employed the boundary element method (BEM) and the Nyström method for discretising the integrals. The iterative algorithm of Kozlov et al. (1991), which reduces the Cauchy problem to solving a sequence of well-posed boundary value problems, was implemented using the BEM for linear elastic materials by Marin et al. (2001), Marin et al. (2002a) and Comino et al. (2007), respectively. Ellabib and Nachaoui (2008) investigated numerically the relaxation of the alternating iterative algorithm of Kozlov et al. (1991), while further investigations were carried out by Marin and Johansson (2010a, 2010b), who also proposed alternative ways of relaxation of both the prescribed displacements and tractions on the over-specified boundary. Moreover, Marin and Johansson (2010a) also proved the convergence of these schemes, introduced appropriate optimal stopping rules and implemented these algorithms with relaxation using the BEM. Huang and Shih (1997) and Marin et al. (2002b) used the CGM, as a result of the variational approach, combined with the BEM in order to solve the two-dimensional Cauchy problem in linear elasticity. The Cauchy problem in elasticity with L^2 -boundary data was approached by combining the BEM with the Landweber–Fridman method and the minimal error method by Marin and Lesnic (2005) and Marin (2009), respectively. Andrieux and Baranger (2008) reformulated the Cauchy problem for three-dimensional elastic media as an energy error minimization problem, with the unknowns given by the surface displacement and traction vectors on the under-specified boundary of the solid. Cimetière et al. (2000) and Cimetière et al. (2001) introduced the so-called fading/evanescent regularization method to solve the Cauchy problem associated with the Laplace equation. This regularization procedure consists of an iterative process, whose convergence was also established (Cimetière et al., 2001; Cimetière et al., 2000). The fading regularization method was numerically implemented, in the case of the Cauchy problem for the Laplace operator, using both the BEM and the FEM by Delvare et al. (2002) and Cimetière et al. (2002), respectively, and it was later extended to solving Cauchy problems in two-dimensional elasticity in conjunction with both the BEM (Delvare and Hanus, 2005) and the FEM (Delvare et al., 2010).

The method of fundamental solutions (MFS) was originally proposed in the early 1960s by Kupradze and Aleksidze (1964) and since its introduction as a numerical method by Mathon and Johnston (1977), it has been successfully applied to a large variety of direct and inverse problems in science and engineering, see e.g. the survey papers by Fairweather and Karageorghis (1998), Golberg and Chen (1999), and Karageorghis et al. (2011). The MFS is a meshless boundary collocation method which belongs to the family of so-called Trefftz methods, may be regarded as an approximation of the indirect BEM (Liu and Šarler, 2014) and is applicable to boundary value problems for which a fundamental solution of the operator in the governing equation is known. In spite of the aforementioned restriction, the MFS has become very popular primarily because of the ease with which it can be implemented, in particular for the solution of problems in complex geometries, as well as its low computational cost.

The aim of this paper is to emphasize and combine the features of the fading regularizing algorithm, originally proposed by Cimetière et al. (2000), Cimetière et al. (2001) and Delvare et al. (2010) for the Laplace equation and the linear elasticity system, respectively, and the MFS in order to obtain a robust, versatile, accurate, stable and convergent iterative procedure for the numerical solution of inverse boundary value problems in two-dimensional linear elasticity, including the Cauchy problem as a particular case. The paper is organized as follows: In Section 2 we formulate mathematically the inverse problems under investigation. The fading regularization method is described in Section 3, whilst the MFS approach for

inverse boundary value problems in two-dimensional isotropic linear elasticity is presented in Section 4. The accuracy, convergence and stability of the numerical results obtained using the MFS in conjunction with the fading regularization method are thoroughly analysed for five inverse boundary value problems associated with two simply and doubly connected two-dimensional geometries in Section 5. Finally, some concluding remarks and possible future work are provided in Section 6.

2. Mathematical formulation

Consider a bounded domain $\Omega \subset \mathbb{R}^2$ occupied by a homogeneous isotropic linear elastic material characterised by Poisson's ratio $\nu \in (0, 0.5)$ and the shear modulus $G > 0$. We also assume that the boundary $\partial\Omega$ of the solution domain Ω is either a smooth or a piecewise smooth curve.

In the absence of body forces, the equilibrium equations of isotropic linear elasticity, in terms of the displacement vector, are given by:

$$\mathcal{L}\mathbf{u}(\mathbf{x}) \equiv -\nabla \cdot \boldsymbol{\sigma}(\mathbf{x}) = \mathbf{0}, \quad \mathbf{x} \in \Omega, \quad (1)$$

where \mathcal{L} is the Lamé or Cauchy–Navier differential operator, $\boldsymbol{\sigma}(\mathbf{x})$ is the stress tensor associated with the displacement vector $\mathbf{u}(\mathbf{x})$, whilst on assuming small deformations, the corresponding strain tensor $\boldsymbol{\epsilon}(\mathbf{x})$ is given by the kinematic relations

$$\boldsymbol{\epsilon}(\mathbf{x}) = \frac{1}{2}(\nabla \mathbf{u}(\mathbf{x}) + \nabla \mathbf{u}(\mathbf{x})^T), \quad \mathbf{x} \in \overline{\Omega} = \Omega \cup \partial\Omega. \quad (2)$$

The stress and strain tensors are related by Hooke's constitutive law, i.e.

$$\boldsymbol{\sigma}(\mathbf{x}) = 2G \left[\boldsymbol{\epsilon}(\mathbf{x}) + \frac{\bar{\nu}}{1-2\bar{\nu}} \text{tr}(\boldsymbol{\epsilon}(\mathbf{x})) \mathbf{I} \right], \quad \mathbf{x} \in \overline{\Omega}, \quad (3)$$

where $\mathbf{I} = [\delta_{ij}]_{1 \leq i, j \leq 2}$ is the identity matrix in $\mathbb{R}^{2 \times 2}$, whilst $\bar{\nu} = \nu$ in the plane strain state and $\bar{\nu} = \nu/(1+\nu)$ in the plane stress state, respectively. The Lamé–Navier differential operator \mathcal{L} in Eq. (1) is obtained by applying the differential operator $-\nabla$ to the constitutive law (3) and then using Eq. (2), i.e.

$$\mathcal{L}\mathbf{u}(\mathbf{x}) \equiv -G \left[\nabla \cdot (\nabla \mathbf{u}(\mathbf{x}) + \nabla \mathbf{u}(\mathbf{x})^T) + \frac{2\bar{\nu}}{1-2\bar{\nu}} \nabla (\nabla \cdot \mathbf{u}(\mathbf{x})) \right]. \quad (4)$$

Further, we let $\mathbf{n}(\mathbf{x})$ be the outward unit normal vector to the boundary $\partial\Omega$ of the solution domain Ω and $\mathbf{t}(\mathbf{x})$ be the traction vector at $\mathbf{x} \in \partial\Omega$ defined by

$$\mathbf{t}(\mathbf{x}) = \boldsymbol{\sigma}(\mathbf{x}) \mathbf{n}(\mathbf{x}), \quad \mathbf{x} \in \partial\Omega. \quad (5)$$

In the direct/forward formulation, the displacement and traction vectors are prescribed on the boundaries $\Gamma_{\mathbf{u}}$ and $\Gamma_{\mathbf{t}}$, respectively, where $\Gamma_{\mathbf{u}} \cup \Gamma_{\mathbf{t}} = \partial\Omega$ and $\Gamma_{\mathbf{u}} \cap \Gamma_{\mathbf{t}} = \emptyset$. In numerous practical situations, only a part of the boundary, say $\Gamma_1 \subset \partial\Omega$, is accessible for measurements, while the remaining boundary part, $\Gamma_2 = \partial\Omega \setminus \Gamma_1$, is inaccessible and hence no boundary data is available on it. In such a situation, additional measurements are available on a portion of or on the entire Γ_1 , hence compensating for the lack of boundary data on Γ_2 , and this corresponds to an inverse boundary value problem.

Let $H^1(\Omega)$ be the Sobolev space of real valued functions in Ω endowed with the usual Sobolev norm. The space of traces functions from $H^1(\Omega)$ to $\partial\Omega$ is denoted by $H^{1/2}(\partial\Omega)$, while the restrictions of the functions belonging to the space $H^{1/2}(\partial\Omega)$ to the subsets $\Gamma_{\mathbf{u}} \subset \partial\Omega$ and $\Gamma_{\mathbf{t}} \subset \partial\Omega$ define the spaces $H^{1/2}(\Gamma_{\mathbf{u}})$ and $H^{1/2}(\Gamma_{\mathbf{t}})$, respectively. Herein, we use the following notation $\mathbf{H}^1(\Omega) := H^1(\Omega) \times H^1(\Omega)$, as well as similar notations for the other function spaces employed, i.e. $\mathbf{H}^{1/2}(\Gamma_{\mathbf{u}}) := H^{1/2}(\Gamma_{\mathbf{u}}) \times H^{1/2}(\Gamma_{\mathbf{u}})$ and $\mathbf{H}^{1/2}(\Gamma_{\mathbf{t}}) := H^{1/2}(\Gamma_{\mathbf{t}}) \times H^{1/2}(\Gamma_{\mathbf{t}})$. Finally, we denote by $\mathbf{H}^{-1/2}(\Gamma_{\mathbf{t}})$ the dual space of $\mathbf{H}^{1/2}(\Gamma_{\mathbf{t}})$.

In the sequel, we consider the following inverse boundary value problem: Find $\mathbf{u} \in \mathbf{H}^1(\Omega)$ such that the governing partial differential Eq. (1) is satisfied together with the boundary conditions:

$$\mathbf{u}(\mathbf{x}) = \tilde{\mathbf{u}}(\mathbf{x}), \quad \mathbf{x} \in \Gamma_{\mathbf{u}}, \quad (6a)$$

and

$$\mathbf{t}(\mathbf{x}) = \tilde{\mathbf{t}}(\mathbf{x}), \quad \mathbf{x} \in \Gamma_{\mathbf{t}}, \quad (6b)$$

where the boundaries $\Gamma_{\mathbf{u}}$ and $\Gamma_{\mathbf{t}}$ satisfy the following relations:

$$\emptyset \neq \Gamma_{\mathbf{u}}, \Gamma_{\mathbf{t}} \subsetneq \partial\Omega; \quad \Gamma_{\mathbf{u}} \cup \Gamma_{\mathbf{t}} \subsetneq \partial\Omega; \quad \Gamma_{\mathbf{u}} \cap \Gamma_{\mathbf{t}} \neq \emptyset; \quad (7)$$

whilst $\tilde{\mathbf{u}} \in \mathbf{H}^{1/2}(\Gamma_{\mathbf{u}})$ and $\tilde{\mathbf{t}} \in \mathbf{H}^{-1/2}(\Gamma_{\mathbf{t}})$. It should be noted that the general inverse boundary value problem in two-dimensional isotropic linear elasticity given by Eqs. (1), (6a), (6b) and (7) actually describes the following cases:

Problem (A): The Cauchy problem in isotropic linear elasticity when $\Gamma_{\mathbf{u}} = \Gamma_{\mathbf{t}}$.

Problem (B): The inverse boundary value problem in isotropic linear elasticity when $\Gamma_{\mathbf{u}} \neq \Gamma_{\mathbf{t}}$.

In Eqs. (6a) and (6b), $\tilde{\mathbf{u}}$ and $\tilde{\mathbf{t}}$ are prescribed boundary displacements and tractions, respectively. Each of the aforementioned inverse problems is considerably more difficult to solve both analytically and numerically than direct problems since its solution does not satisfy the general conditions of well-posedness (Hadamard, 1923). Therefore, direct methods, such as the least-squares method, will fail to produce stable and physically meaningful solutions to these problems and hence suitable regularization procedures should be employed.

3. Fading regularization method

In this section, we consider the Cauchy problem (A) given by Eqs. (1), (6a) and (6b) with $\Gamma := \Gamma_{\mathbf{u}} = \Gamma_{\mathbf{t}}$. To describe the fading regularization method, originally proposed by Cimetière et al. (2000) and Cimetière et al. (2001), we define the space of solutions of the equilibrium equations of isotropic linear elasticity (1) by

$$\mathbf{H}(\Omega) = \{\mathbf{u} \in \mathbf{H}^1(\Omega) \mid \mathcal{L}\mathbf{u}(\mathbf{x}) = \mathbf{0}, \mathbf{x} \in \Omega, \text{ in a weak sense}\}. \quad (8)$$

As a direct consequence of definition (8), the traces of elements $\mathbf{u} \in \mathbf{H}(\Omega)$ on $\partial\Omega$, $(\mathbf{u}|_{\partial\Omega}, \mathbf{t}(\mathbf{u})|_{\partial\Omega})$, where $\mathbf{t}(\mathbf{u})|_{\partial\Omega} := (\boldsymbol{\sigma}(\mathbf{u})\mathbf{n})|_{\partial\Omega}$ is the traction vector on $\partial\Omega$ (i.e. the Neumann boundary condition) corresponding to the displacement vector $\mathbf{u}|_{\partial\Omega}$, generate the space of compatible data on $\partial\Omega$, namely

$$\mathbf{H}(\partial\Omega) = \{\mathbf{U} = (\mathbf{u}, \mathbf{t}(\mathbf{u})) \in \mathbf{H}^{1/2}(\partial\Omega) \times \mathbf{H}^{-1/2}(\partial\Omega) \mid \exists \mathbf{v} \in \mathbf{H}(\Omega) : \mathbf{v}|_{\partial\Omega} = \mathbf{u}, \mathbf{t}(\mathbf{v})|_{\partial\Omega} = \mathbf{t}(\mathbf{u})\}. \quad (9)$$

It can be easily shown that the space of compatible data $\mathbf{H}(\partial\Omega)$ is a closed subspace of $\mathbf{H}^{1/2}(\partial\Omega) \times \mathbf{H}^{-1/2}(\partial\Omega)$ with respect to the scalar product

$$\begin{aligned} \langle \mathbf{U}, \mathbf{V} \rangle_{\mathbf{H}(\partial\Omega)} &= \int_{\partial\Omega} \mathbf{u}(\mathbf{x}) \cdot \mathbf{v}(\mathbf{x}) \, d\Gamma(\mathbf{x}) \\ &\quad + \frac{1}{G^2} \int_{\partial\Omega} \mathbf{t}(\mathbf{u}(\mathbf{x})) \cdot \mathbf{t}(\mathbf{v}(\mathbf{x})) \, d\Gamma(\mathbf{x}), \quad (10) \\ \forall \mathbf{U} &= (\mathbf{u}, \mathbf{t}(\mathbf{u})), \mathbf{V} = (\mathbf{v}, \mathbf{t}(\mathbf{v})) \in \mathbf{H}(\partial\Omega). \end{aligned}$$

Analogously, one can define the space of restrictions on Γ of the space of compatible data $\mathbf{H}(\partial\Omega)$, denoted by $\mathbf{H}(\Gamma)$, which is endowed with the scalar product on $\mathbf{H}(\partial\Omega)$ defined by (10) and its induced norm $\|\cdot\|_{\mathbf{H}(\Gamma)}$.

The Cauchy problem (A), given by Eqs. (1), (6a), (6b) and $\Gamma := \Gamma_{\mathbf{u}} = \Gamma_{\mathbf{t}}$, can be re-written in an equivalent form as follows:

$$\begin{aligned} &|\text{Given } \tilde{\mathbf{U}} = (\tilde{\mathbf{u}}, \tilde{\mathbf{t}}) \in \mathbf{H}(\Gamma), \\ &\text{find } \mathbf{U} = (\mathbf{u}, \mathbf{t}(\mathbf{u})) \in \mathbf{H}(\partial\Omega) : \quad \mathbf{U}|_{\Gamma} = \tilde{\mathbf{U}}. \end{aligned} \quad (11)$$

It should be noted that problem (11) is in general not solvable unless the given Cauchy data are compatible, i.e. $\tilde{\mathbf{U}} \in \mathbf{H}(\Gamma)$. If a solution of problem (11) exists, then it is unique but does not depend continuously on the data, i.e. problem (11) is ill-posed in the sense of Hadamard (1923). Consequently, this inverse problem should be regularized in order to obtain a stable and physically meaningful solution of it and this is achieved by employing the fading regularization method.

The fading regularization method was originally proposed by Cimetière et al. (2000) and Cimetière et al. (2001) for solving the Cauchy problem associated with the Laplace equation and later extended to Cauchy problems in linear elasticity by Delvare et al. (2010). Further, we briefly describe the principle of the fading regularization method. The idea for solving problem (11) consists of seeking the best solution satisfying the boundary conditions (6a) and (6b) on the accessible boundary, provided that the equilibrium Eq. (1) are fulfilled. This leads to defining the solution of Cauchy problem (1), (6a) and (6b) in terms of an approximate solution which solves the following optimisation problem:

$$\begin{aligned} &|\text{Given } \tilde{\mathbf{U}} = (\tilde{\mathbf{u}}, \tilde{\mathbf{t}}) \in \mathbf{H}(\Gamma), \text{ find } \mathbf{U} = (\mathbf{u}, \mathbf{t}(\mathbf{u})) \in \mathbf{H}(\partial\Omega) : \\ &\quad J(\mathbf{U}) \leq J(\mathbf{V}), \forall \mathbf{V} = (\mathbf{v}, \mathbf{t}(\mathbf{v})) \in \mathbf{H}(\partial\Omega), \end{aligned} \quad (12a)$$

where

$$J(\cdot) : \mathbf{H}(\partial\Omega) \longrightarrow [0, \infty), \quad J(\mathbf{V}) = \|\mathbf{V} - \tilde{\mathbf{U}}\|_{\mathbf{H}(\Gamma)}^2. \quad (12b)$$

We note that problem (12) is ill-posed. Actually, it is always possible to find a solution $\mathbf{U} \in \mathbf{H}(\partial\Omega)$ such that its restriction to Γ is as close as possible to the given data $\tilde{\mathbf{U}}$, while its restriction to $\partial\Omega \setminus \Gamma$ is unstable. Therefore, it is necessary to introduce a control term in the functional J to overcome this instability of the solution. Hence the optimisation problem (12) is replaced by the following one:

$$\begin{aligned} &|\text{Given } \tilde{\mathbf{U}} = (\tilde{\mathbf{u}}, \tilde{\mathbf{t}}) \in \mathbf{H}(\Gamma), \text{ find } \mathbf{U} = (\mathbf{u}, \mathbf{t}(\mathbf{u})) \in \mathbf{H}(\partial\Omega) : \\ &\quad J_{\lambda}(\mathbf{U}) \leq J_{\lambda}(\mathbf{V}), \forall \mathbf{V} = (\mathbf{v}, \mathbf{t}(\mathbf{v})) \in \mathbf{H}(\partial\Omega), \end{aligned} \quad (13a)$$

where

$$\begin{aligned} &J_{\lambda}(\cdot) : \mathbf{H}(\partial\Omega) \longrightarrow [0, \infty), \\ &J_{\lambda}(\mathbf{V}) = \|\mathbf{V} - \tilde{\mathbf{U}}\|_{\mathbf{H}(\Gamma)}^2 + \lambda \|\mathbf{V} - \Phi\|_{\mathbf{H}(\partial\Omega)}^2. \end{aligned} \quad (13b)$$

Here $\lambda > 0$ is a parameter to be specified, $\Phi \in \mathbf{H}(\partial\Omega)$, whilst the norms $\|\cdot\|_{\mathbf{H}(\partial\Omega)}$ and $\|\cdot\|_{\mathbf{H}(\Gamma)}$ are the norms derived from the scalar product on $\mathbf{H}(\partial\Omega)$ defined by Eq. (10) and the corresponding scalar product induced on $\mathbf{H}(\Gamma)$, respectively. The control term $\|\mathbf{V} - \Phi\|_{\mathbf{H}(\partial\Omega)}^2$ in (13b) is defined on the entire boundary $\partial\Omega$ and may be considered as a regularizing term. The introduction of this control term makes problem (13) well-posed in the sense of Hadamard (1923) and, in particular, its solution depends continuously on the data $\tilde{\mathbf{U}}$, as well as the coefficient λ and the choice of Φ .

One way to obtain a solution to the Cauchy problem (1), (6a) and (6b), which is also independent of λ or Φ , is to introduce this solution, or the solution of optimization problem (12), as the limit of a sequence of well-posed optimization problems (13). Consequently, an iterative regularizing strategy is introduced (Cimetière et al., 2001; Cimetière et al., 2000) and this makes the solution of problem (11) the fix point of an operator defined on $\mathbf{H}(\partial\Omega)$ and also taking values in $\mathbf{H}(\partial\Omega)$ or, equivalently, each iterate is the solution of a well-posed optimisation problem. More precisely, the corresponding iterative algorithm reads as follows:

Step 1: Choose the initial guess $\mathbf{U}^{(0)} = 0$.

Step 2: For each $k \geq 1$, solve the following minimization problem:

$$\left\{ \begin{array}{l} \text{Find } \mathbf{U}^{(k)} \in \mathbf{H}(\partial\Omega) : J_{\lambda}^{k-1}(\mathbf{U}^{(k)}) \leq J_{\lambda}^{k-1}(\mathbf{V}), \forall \mathbf{V} \in \mathbf{H}(\partial\Omega), \\ \text{where } J_{\lambda}^{k-1}(\cdot) : \mathbf{H}(\partial\Omega) \rightarrow [0, \infty), \\ J_{\lambda}^{k-1}(\mathbf{V}) = \|\mathbf{V} - \tilde{\mathbf{U}}\|_{\mathbf{H}(\Gamma)}^2 + \lambda \|\mathbf{V} - \mathbf{U}^{(k-1)}\|_{\mathbf{H}(\partial\Omega)}^2. \end{array} \right. \quad (14)$$

Clearly, the aforementioned iterative procedure can also be written in the following equivalent form:

Step 1: Choose the initial guess $\mathbf{U}^{(0)} = 0$.

Step 2: For each $k \geq 1$, solve the following problem:

$$\left\{ \begin{array}{l} \text{Find } \mathbf{U}^{(k)} \in \mathbf{H}(\partial\Omega) : \\ \langle \mathbf{U}^{(k)} - \tilde{\mathbf{U}}, \mathbf{V} \rangle_{\mathbf{H}(\Gamma)} + \lambda \langle \mathbf{U}^{(k)} - \mathbf{U}^{(k-1)}, \mathbf{V} \rangle_{\mathbf{H}(\partial\Omega)} = 0, \\ \forall \mathbf{V} \in \mathbf{H}(\partial\Omega). \end{array} \right. \quad (15)$$

This iterative process accounts, in a very good and precise manner, for the equilibrium Eq. (1) since at each iteration the optimal element is sought in the Sobolev space $\mathbf{H}(\partial\Omega)$, see Eqs. (13)–(15). The minimising functional in (13b) or (14) consists of two terms, each of these having its own role. More precisely, the first term of the functional given by (13b) or (14) is defined on Γ only and measures the gap between the sought optimal element in $\mathbf{H}(\partial\Omega)$ and the given over-specified boundary conditions on Γ . The second term of the functional from Eqs. (13b) or (14) is a regularization term and is defined not only on the under-specified boundary $\partial\Omega \setminus \Gamma$, where the boundary data are reconstructed, but on the entire boundary $\partial\Omega$ of the solution domain, with the mention that this term controls the distance between the new optimal element sought at the present iteration and that obtained at the previous iteration. It should be noted that the norm of the regularization term decreases and tends to zero as the number of iterations increases. Hence at each iteration, the optimal element satisfies the equilibrium equations (1) and agrees as well as possible with the over-specified boundary data $\tilde{\mathbf{U}}|_{\Gamma}$, while at the same time remains close to the optimal element obtained at the previous iteration. Finally, we stress out that the proposed fading regularization algorithm allows for both the reconstruction of the missing boundary data on the under-specified boundary $\partial\Omega \setminus \Gamma$ and the denoising of the perturbed over-specified boundary data on Γ .

4. Method of fundamental solutions (MFS)

For any collocation point $\mathbf{x} \in \bar{\Omega}$ and any singularity or source point $\boldsymbol{\xi} \in \mathbb{R}^2 \setminus \bar{\Omega}$, the fundamental solution matrix $\mathbf{U}(\mathbf{x}, \boldsymbol{\xi}) = [U_{ij}(\mathbf{x}, \boldsymbol{\xi})]_{i,j=1,2}$, for the displacement vector in the Cauchy–Navier system in two-dimensional isotropic linear elasticity is given by:

$$U_{ij}(\mathbf{x}, \boldsymbol{\xi}) = \frac{1}{8\pi G(1-\nu)} \left[-(3-4\nu) \log \|\mathbf{x} - \boldsymbol{\xi}\| \delta_{ij} + \frac{x_i - \xi_i}{\|\mathbf{x} - \boldsymbol{\xi}\|} \frac{x_j - \xi_j}{\|\mathbf{x} - \boldsymbol{\xi}\|} \right], \quad i, j = 1, 2. \quad (16)$$

By taking $\mathbf{x} \in \partial\Omega$ and differentiating Eq. (16) with respect to x_j , $j = 1, 2$, one obtains, in a straightforward manner, the derivatives of the fundamental solution for the displacement vector. Further, by combining Eq. (16) with the definition of the traction vector (5) and Hooke's constitutive law (3) of isotropic linear elasticity, the fundamental solution matrix $\mathbf{T}(\mathbf{x}, \boldsymbol{\xi}) = [T_{ij}(\mathbf{x}, \boldsymbol{\xi})]_{i,j=1,2}$, for the traction vector in the case of two-dimensional isotropic linear elasticity is then obtained. More precisely, one obtains:

$$\begin{aligned} T_{1j}(\mathbf{x}, \boldsymbol{\xi}) &= \frac{2G}{1-2\nu} \left[(1-\nu) \frac{\partial U_{1j}(\mathbf{x}, \boldsymbol{\xi})}{\partial x_1} + \nu \frac{\partial U_{2j}(\mathbf{x}, \boldsymbol{\xi})}{\partial x_2} \right] n_1(\mathbf{x}) \\ &+ G \left[\frac{\partial U_{1j}(\mathbf{x}, \boldsymbol{\xi})}{\partial x_2} + \frac{\partial U_{2j}(\mathbf{x}, \boldsymbol{\xi})}{\partial x_1} \right] n_2(\mathbf{x}), \quad j = 1, 2, \end{aligned} \quad (17a)$$

$$\begin{aligned} T_{2j}(\mathbf{x}, \boldsymbol{\xi}) &= G \left[\frac{\partial U_{1j}(\mathbf{x}, \boldsymbol{\xi})}{\partial x_2} + \frac{\partial U_{2j}(\mathbf{x}, \boldsymbol{\xi})}{\partial x_1} \right] n_1(\mathbf{x}) \\ &+ \frac{2G}{1-2\nu} \left[\nu \frac{\partial U_{1j}(\mathbf{x}, \boldsymbol{\xi})}{\partial x_1} + (1-\nu) \frac{\partial U_{2j}(\mathbf{x}, \boldsymbol{\xi})}{\partial x_2} \right] n_2(\mathbf{x}), \\ j &= 1, 2. \end{aligned} \quad (17b)$$

In the MFS, the displacement vector is approximated by a linear combination of fundamental solution matrices with respect to N sources, $\{\boldsymbol{\xi}^{(n)}\}_{n=1,N} \subset \mathbb{R}^2 \setminus \bar{\Omega}$, in the form (Fairweather and Karageorghis, 1998)

$$\mathbf{u}(\mathbf{x}) \approx \mathbf{u}_N(\mathbf{c}, \boldsymbol{\xi}; \mathbf{x}) = \sum_{n=1}^N \mathbf{U}(\mathbf{x}, \boldsymbol{\xi}^{(n)}) \mathbf{c}^{(n)}, \quad \mathbf{x} \in \bar{\Omega}, \quad (18)$$

where the vector $\mathbf{c} = (c_1^{(1)}, c_2^{(1)}, c_1^{(2)}, c_2^{(2)}, \dots, c_1^{(N)}, c_2^{(N)})^T \in \mathbb{R}^{2N}$ contains the unknown MFS coefficients, $\boldsymbol{\xi} \in \mathbb{R}^{2N}$ is a vector containing the coordinates of the sources and the components of the fundamental solution matrix $\mathbf{U}(\mathbf{x}, \boldsymbol{\xi}^{(n)})$ are given by Eq. (16). Analogously to Eq. (18), one can also approximate the traction vector on $\partial\Omega$ by a linear combination of fundamental solution matrices with respect to the sources $\{\boldsymbol{\xi}^{(n)}\}_{n=1,N}$ as (Fairweather and Karageorghis, 1998)

$$\mathbf{t}(\mathbf{x}) \approx \mathbf{t}_N(\mathbf{c}, \boldsymbol{\xi}; \mathbf{x}) = \sum_{n=1}^N \mathbf{T}(\mathbf{x}, \boldsymbol{\xi}^{(n)}) \mathbf{c}^{(n)}, \quad \mathbf{x} \in \partial\Omega, \quad (19)$$

where the components of the fundamental solution matrix $\mathbf{T}(\mathbf{x}, \boldsymbol{\xi}^{(n)})$ are given by Eqs. (17a) and (17b).

Further, according to the fading regularization algorithm described in Section 3, at each step $k \geq 0$ of the minimization problem (13) or, equivalently, Eq. (14), one has to approximate both the known boundary data $\mathbf{u}^{(k)}|_{\Gamma_u}$ and $\mathbf{t}^{(k)}|_{\Gamma_t}$ and the unknown boundary data $\mathbf{u}^{(k)}|_{\partial\Omega \setminus \Gamma_u}$ and $\mathbf{t}^{(k)}|_{\partial\Omega \setminus \Gamma_t}$, at the same time accounting for the given perturbed boundary conditions $\tilde{\mathbf{u}}^\varepsilon|_{\Gamma_u}$ and $\tilde{\mathbf{t}}^\varepsilon|_{\Gamma_t}$. To do this, we collocate the corresponding boundary conditions (6a) and (6b) at the points $\{\mathbf{x}^{(m)}\}_{m=1,M_u}$ on Γ_u and $\{\mathbf{x}^{(m')}\}_{m'=1,M_t}$ on Γ_t and also express the MFS approximations (18) and (19) for the unknown displacements and tractions at the points $\{\mathbf{x}^{(m)}\}_{m=M_u+1,M}$ on $\partial\Omega \setminus \Gamma_u$ and $\{\mathbf{x}^{(m')}\}_{m'=M_t+1,M}$ on $\partial\Omega \setminus \Gamma_t$, respectively. Consequently, at each step $k \geq 0$, the minimization problem (13) or, equivalently, Eq. (14), is reduced to a linear minimisation problem with respect to the corresponding unknown MFS constants.

5. Numerical results and discussion

In this section, we apply the fading regularization method described in Section 3, in conjunction with the MFS presented in Section 4, to five inverse problems for two test examples in two dimensions. More precisely, we solve the inverse problems (A) and (B) in a doubly connected domains with a smooth boundary and a simply connected domain with a piecewise smooth boundary, respectively, for an isotropic linear elastic material characterised by the shear modulus $G = 4.80 \times 10^{10}$ N/m² and Poisson's ratio $\nu = 0.34$ and corresponding to a copper alloy.

5.1. Examples

Example 1 (Doubly connected domain with a smooth boundary). We consider the Cauchy problem (A) in the annular domain $\Omega = \{\mathbf{x} \in \mathbb{R}^2 \mid R_{\text{int}} < \|\mathbf{x}\| < R_{\text{out}}\}$, where $R_{\text{int}} = 1.0$ and $R_{\text{out}} = 2.0$, which is bounded by the inner and outer boundaries $\Gamma_{\text{int}} = \{\mathbf{x} \in \mathbb{R}^2 \mid \|\mathbf{x}\| = R_{\text{int}}\}$ and $\Gamma_{\text{out}} = \{\mathbf{x} \in \mathbb{R}^2 \mid \|\mathbf{x}\| = R_{\text{out}}\}$, respectively. We also consider the following analytical solution in displacements which describe a plane strain state

$$\mathbf{u}^{(\text{an})}(\mathbf{x}) = \left[\nu \left(\frac{1-\nu}{1+\nu} \right) - \nu \frac{1}{\|\mathbf{x}\|^2} \right] \frac{\mathbf{x}}{2G}, \quad \mathbf{x} \in \bar{\Omega}, \quad (20a)$$

where

$$\begin{aligned} \nu &\equiv -\frac{\sigma_{\text{out}} R_{\text{out}}^2 - \sigma_{\text{int}} R_{\text{int}}^2}{R_{\text{out}}^2 - R_{\text{int}}^2} \quad \text{and} \\ W &\equiv \frac{(\sigma_{\text{out}} - \sigma_{\text{int}}) R_{\text{out}}^2 R_{\text{int}}^2}{R_{\text{out}}^2 - R_{\text{int}}^2}. \end{aligned} \quad (20b)$$

which correspond to constant inner and outer radial pressures where $\sigma_{\text{int}} = 1.0 \times 10^{10} \text{ N/m}^2$ and $\sigma_{\text{out}} = 2.0 \times 10^{10} \text{ N/m}^2$. Here we consider the following cases:

- (i) $\Gamma_{\mathbf{u}} = \Gamma_{\mathbf{t}} = \Gamma_{\text{out}}$;
- (ii) $\Gamma_{\mathbf{u}} = \Gamma_{\mathbf{t}} = \Gamma_{\text{int}}$.

Example 2 (Simply connected domain with a piecewise smooth boundary). We consider the inverse boundary value problem (B) in the unit square $\Omega = (-0.5, 0.5)^2$ and the following analytical solution in displacements

$$\mathbf{u}^{(\text{an})}(\mathbf{x}) = \frac{\sigma_0}{2G(1+\nu)} \begin{bmatrix} x_1 \\ -\nu x_2 \end{bmatrix} + \frac{\tau_0}{G} \begin{bmatrix} x_2 \\ 0 \end{bmatrix}, \quad \mathbf{x} \in \bar{\Omega}, \quad (21a)$$

which corresponds to a combined uniform traction and pure shear stress given by

$$\boldsymbol{\sigma}^{(\text{an})}(\mathbf{x}) = \begin{bmatrix} \sigma_0 & \tau_0 \\ \tau_0 & 0 \end{bmatrix}, \quad \mathbf{x} \in \bar{\Omega}, \quad (21b)$$

where $\sigma_0 = \tau_0 = 1.0 \times 10^{10} \text{ N/m}^2$. Here, we consider the following cases:

- (i) $\Gamma_{\mathbf{u}} = \Gamma_{\mathbf{t}} = [-0.5, 0.5] \times \{\pm 0.5\} \cup \{0.5\} \times (-0.5, 0.5)$;
- (ii) $\Gamma_{\mathbf{u}} = [-0.5, 0.5] \times \{-0.5\} \cup \{0.5\} \times (-0.5, 0.5)$ and $\Gamma_{\mathbf{t}} = \Gamma_{\mathbf{u}} \cup [-0.5, 0.5] \times \{0.5\}$;
- (iii) $\Gamma_{\mathbf{u}} = [-0.5, 0.5] \times \{-0.5\}$ and $\Gamma_{\mathbf{t}} = \Gamma_{\mathbf{u}} \cup [-0.5, 0.5] \times \{0.5\} \cup \{0.5\} \times (-0.5, 0.5)$.

It should be mentioned that, for this example, the Cauchy problem (A) as given by case (i) actually represents a limiting case of the general inverse boundary value problem (B).

In all examples we have taken $M_{\mathbf{u}}$ and $M_{\mathbf{t}}$ uniformly distributed collocation points on $\Gamma_{\mathbf{u}}$ and $\Gamma_{\mathbf{t}}$, respectively, as well as N uniformly distributed sources associated with the entire boundary $\partial\Omega$ of the solution domain Ω . It should be mentioned that the sources are pre-assigned and kept fixed throughout the solution process (i.e. the so-called static MFS approach has been employed) on a pseudo-boundary $\partial\tilde{\Omega}$ of a similar shape to that of $\partial\Omega$ such that $\text{dist}(\partial\tilde{\Omega}, \partial\Omega)$ is a fixed constant (Gorzelańczyk and Kołodziej, 2008). According to the notations used in Section 4, the corresponding MFS parameters have been set as follows:

- (a) Example 1: $N_{\text{out}} \in \{40; 80\}$ and $N_{\text{int}} = N_{\text{out}}/2$ on $\tilde{\Gamma}_{\text{out}}$ and $\tilde{\Gamma}_{\text{int}}$, respectively, such that $N = N_{\text{out}} + N_{\text{int}}$, where $\tilde{\Omega} = \{\mathbf{x} \in \mathbb{R}^2 \mid R_{\text{int}} - d_1 < \|\mathbf{x}\| < R_{\text{out}} + d_1\}$, $\partial\tilde{\Omega} = \tilde{\Gamma}_{\text{out}} \cup \tilde{\Gamma}_{\text{int}}$, $d_1 > 0$ and $d_2 = 0.5$, whilst $M_{\mathbf{u}} = M_{\mathbf{t}} \in \{40; 80\}$ on $\Gamma_{\mathbf{u}} = \Gamma_{\mathbf{t}} = \Gamma_{\text{out}}$ in the case of the first Cauchy problem considered and $M_{\mathbf{u}} = M_{\mathbf{t}} \in$

$\{20; 40\}$ on $\Gamma_{\mathbf{u}} = \Gamma_{\mathbf{t}} = \Gamma_{\text{int}}$ for the second Cauchy problem investigated.

- (b) Example 2: $N = 80$ on $\partial\tilde{\Omega}$, where $\tilde{\Omega} = (-0.5 - d, 0.5 + d)^2$ and $d > 0$, whilst $M_{\mathbf{t}} = 3N/4$ on $\Gamma_{\mathbf{t}}$ and $M_{\mathbf{u}} = \ell N/4$ on $\Gamma_{\mathbf{u}}$, $\ell \in \{1, 2, 3\}$, for the corresponding cases (i)–(iii), respectively.

In order to simulate the inherent measurement errors, we consider that the boundary data corresponding to the inverse problems investigated herein is noisy. More precisely, we assume that the given exact boundary data $\tilde{\mathbf{u}}|_{\Gamma_{\mathbf{u}}} = \mathbf{u}^{(\text{an})}|_{\Gamma_{\mathbf{u}}}$ and/or $\tilde{\mathbf{t}}|_{\Gamma_{\mathbf{t}}} = \mathbf{t}^{(\text{an})}|_{\Gamma_{\mathbf{t}}}$ has been perturbed as

$$\tilde{\mathbf{u}}^{\varepsilon}(\mathbf{x}) = (1 + p_{\mathbf{u}}\rho) \mathbf{u}^{(\text{an})}(\mathbf{x}), \quad \mathbf{x} \in \Gamma_{\mathbf{u}}, \quad (22a)$$

$$\tilde{\mathbf{t}}^{\varepsilon}(\mathbf{x}) = (1 + p_{\mathbf{t}}\rho) \mathbf{t}^{(\text{an})}(\mathbf{x}), \quad \mathbf{x} \in \Gamma_{\mathbf{t}}, \quad (22b)$$

where $p_{\mathbf{u}}$ and $p_{\mathbf{t}}$ are the levels of percentage noise added to $\tilde{\mathbf{u}}|_{\Gamma_{\mathbf{u}}} = \mathbf{u}^{(\text{an})}|_{\Gamma_{\mathbf{u}}}$ and/or $\tilde{\mathbf{t}}|_{\Gamma_{\mathbf{t}}} = \mathbf{t}^{(\text{an})}|_{\Gamma_{\mathbf{t}}}$, respectively, and ρ is a pseudo-random number drawn from the standard uniform distribution on the interval $[-1, 1]$ generated using the MATLAB command $-1 + 2 * \text{rand}(\cdot)$.

To assess the accuracy and convergence of the fading regularization MFS algorithm, for any vector-valued function $\mathbf{f} = [f_1, \dots, f_{\ell}]^T : \Gamma \rightarrow \mathbb{R}^{\ell}$, where $\Gamma = \partial\Omega \setminus \Gamma_{\mathbf{u}}$ or $\Gamma = \partial\Omega \setminus \Gamma_{\mathbf{t}}$, and any set of points $\{\mathbf{x}^{(n)}\}_{n=1, N_{\Gamma}} \subset \Gamma$, we introduce the following *relative root mean square (RMS) error* of \mathbf{f} on Γ :

$$e_{\Gamma}(\mathbf{f}) = \sqrt{\frac{\frac{1}{N_{\Gamma}} \sum_{n=1}^{N_{\Gamma}} \sum_{j=1}^{\ell} [f_j^{(\text{num})}(\mathbf{x}^{(n)}) - f_j(\mathbf{x}^{(n)})]^2}{\frac{1}{N_{\Gamma}} \sum_{n=1}^{N_{\Gamma}} \sum_{j=1}^{\ell} f_j(\mathbf{x}^{(n)})^2}}, \quad (23)$$

where $f_j^{(\text{num})}(\mathbf{x})$, $j = 1, \dots, \ell$, denotes an approximate numerical value for $f_j(\mathbf{x})$, $j = 1, \dots, \ell$, for $\mathbf{x} \in \Gamma$. Clearly, herein $\ell = 2$.

5.2. Stopping criterion

Fig. 1(a) and (b) present the evolution of the relative RMS errors $e_{\partial\Omega \setminus \Gamma_{\mathbf{u}}}(\mathbf{u})$ and $e_{\partial\Omega \setminus \Gamma_{\mathbf{t}}}(\mathbf{t})$, respectively, as functions of the number of iterations k , when applying the fading regularization method presented in Section 3, in conjunction with the MFS briefly described in Section 4, $M_{\mathbf{u}} = M_{\mathbf{t}} = 40$, $N_{\text{out}} = 40$, $N_{\text{int}} = 20$, $d_1 = d_2 = 0.5$, $\lambda = 1.0 \times 10^{-2}$, $p_{\mathbf{u}} \in \{1\%, 3\%, 5\%$ and $p_{\mathbf{t}} = 0$, for the Cauchy problem (A) associated with the Example 1, case (i). It can be seen from these figures that both these errors attain their corresponding minimum for about the same number of iterations k , after which they start increasing either very slowly ($e_{\partial\Omega \setminus \Gamma_{\mathbf{u}}}(\mathbf{u})$) or very rapidly ($e_{\partial\Omega \setminus \Gamma_{\mathbf{t}}}(\mathbf{t})$). Hence the combined MFS fading regularization algorithm should be stabilised by stopping it at the aforementioned value of k and this is achieved by introducing an appropriate stopping criterion.

As can be seen from Fig. 1(c) and (d), a good option for the required stopping criterion would be to cease the iterative procedure when the relative RMS errors (23) for the known displacement $\mathbf{u}|_{\Gamma_{\mathbf{u}}}$ and traction vectors $\mathbf{t}|_{\Gamma_{\mathbf{t}}}$, respectively, attain their corresponding minimum. However, since the fading regularization method presented in Section 3 may be viewed as a generalization of the classical Tikhonov regularization method applied to the continuous inverse problem under investigation, we prefer to employ another stopping criterion, which is rigorous and, at the same time, has a mathematical rationale, namely the discrepancy principle of Morozov (1966).

To do so, we introduce the convergence error E defined by

$$E(k) := \|\mathbf{U}^{(k)}|_{\Gamma} - \tilde{\mathbf{U}}^{\varepsilon}\|_2, \quad (24a)$$

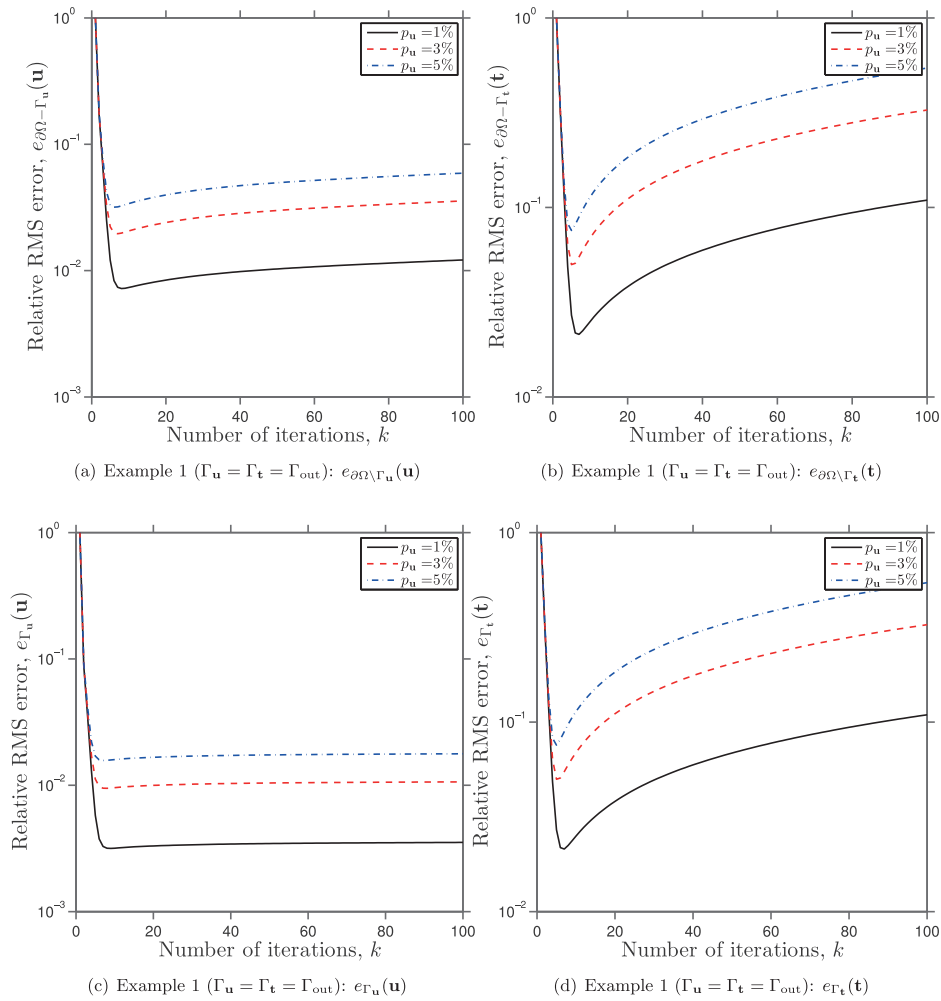


Fig. 1. The relative RMS errors (a) $e_{\partial\Omega\backslash\Gamma_u}(\mathbf{u})$, (b) $e_{\partial\Omega\backslash\Gamma_t}(\mathbf{t})$, (c) $e_{\Gamma_u}(\mathbf{u})$ and (d) $e_{\Gamma_t}(\mathbf{t})$, as functions of the number of iterations, k , obtained using the fading regularization MFS algorithm, $M_u = M_t = 40$, $N_{out} = 40$, $N_{int} = 20$, $d_1 = d_2 = 0.5$, $\lambda = 1.0 \times 10^{-2}$, $p_u \in \{1\%, 3\%, 5\% \}$ and $p_t = 0$, for the Cauchy problem (A) given by Example 1 with $\Gamma_u = \Gamma_t = \Gamma_{out}$, i.e. case (i).

where $\tilde{\mathbf{U}}^\varepsilon$ and $\mathbf{U}^{(k)}|_\Gamma$ are the measured noisy data and the computed data at step k of the iterative procedure on the boundary Γ , respectively. Note that the convergence error introduced above actually measures the fit of the numerical solution at step k into the discrete MFS system and represents the discretised version of the first term in the minimisation functional J_λ^{k-1} given by Eq. (13). The discrepancy principle (Morozov, 1966) states that the iterative procedure should be stopped at the first iteration, k_{opt} , when the convergence error has about the same order as the noise in the data, namely

$$k_{opt} = \min \{k \geq 1 \mid E(k) \leq \varepsilon\}, \quad (24b)$$

where $\varepsilon = \|\tilde{\mathbf{u}}^\varepsilon|_{\Gamma_u} - \tilde{\mathbf{u}}|_{\Gamma_u}\|_2 + \|\tilde{\mathbf{t}}^\varepsilon|_{\Gamma_t} - \tilde{\mathbf{t}}|_{\Gamma_t}\|_2$ is a discrete measure of the noise in the prescribed data.

Fig. 2 displays the convergence error E defined by Eq. (24a) as a function of the number of iterations k , obtained using $M_u = M_t = 40$, $N_{out} = 40$, $N_{int} = 20$, $d_1 = d_2 = 0.5$, $\lambda = 1.0 \times 10^{-2}$, and various levels of noise added to $\mathbf{u}|_{\Gamma_u}$, for the Cauchy problem (i) associated with the Example 1, as well as the corresponding values of ε (the dotted lines). By comparing Figs. 1(a), (b) and 2, it can be concluded that Morozov's discrepancy principle (24b) yields a good approximation for the minimum of the relative RMS accuracy errors $e_{\partial\Omega\backslash\Gamma_u}(\mathbf{u})$ and $e_{\partial\Omega\backslash\Gamma_t}(\mathbf{t})$ and, consequently, has a stabilising effect on the iterative procedure given by the fading regularization MFS algorithm presented herein.

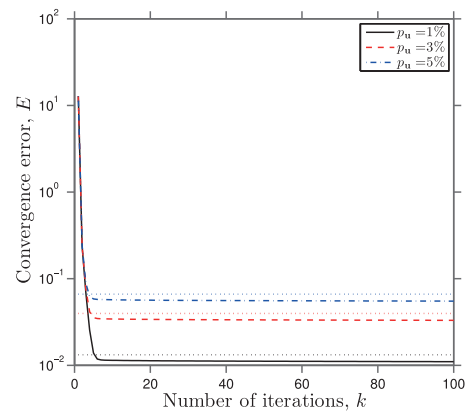


Fig. 2. The convergence error $E(k) = \|\mathbf{U}^{(k)}|_\Gamma - \tilde{\mathbf{U}}^\varepsilon\|_2$, as a function of the number of iterations k and the corresponding $\varepsilon(\dots)$ given by Morozov's discrepancy principle, obtained using the fading regularization MFS algorithm, $M_u = M_t = 40$, $N_{out} = 40$, $N_{int} = 20$, $d_1 = d_2 = 0.5$, $\lambda = 1.0 \times 10^{-2}$, $p_u \in \{1\%, 3\%, 5\% \}$ and $p_t = 0$, for the Cauchy problem (A) given by Example 1 with $\Gamma_u = \Gamma_t = \Gamma_{out}$, i.e. case (i).

5.3. Convergence and stability

Fig. 3(a) and (b) show the exact and numerical displacements u_1 and u_2 on the under-specified boundary $\partial\Omega\backslash\Gamma_u$, respectively,

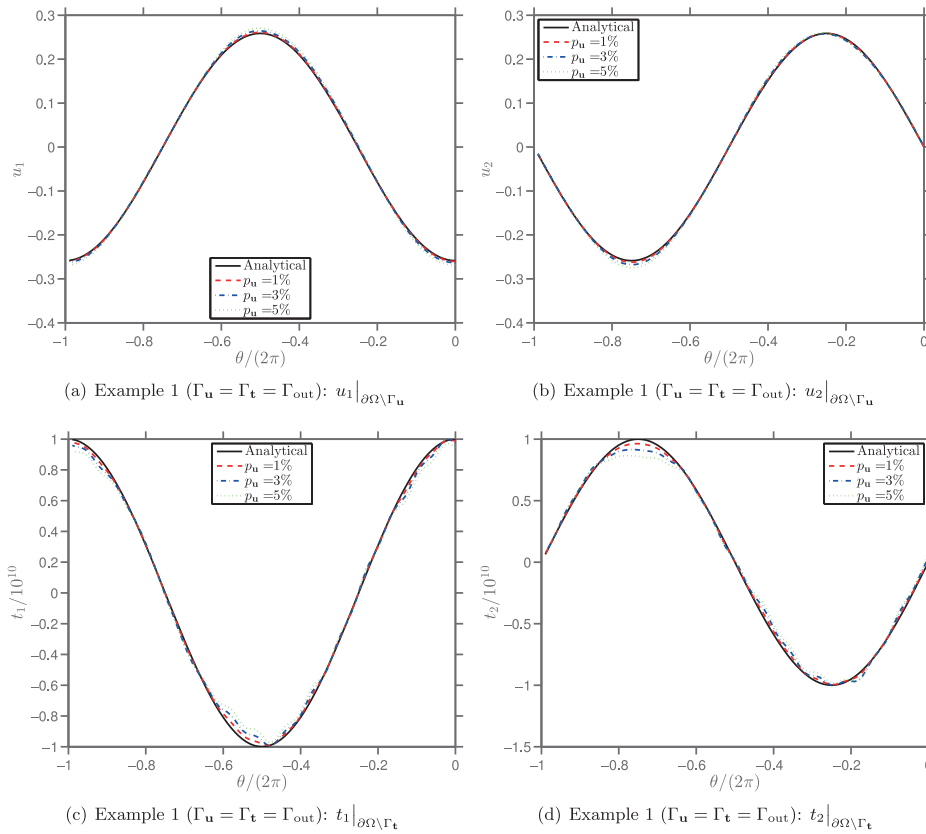


Fig. 3. The analytical and numerical displacements (a) $u_1|_{\partial\Omega\setminus\Gamma_u}$ and (b) $u_2|_{\partial\Omega\setminus\Gamma_u}$, and tractions (c) $t_1|_{\partial\Omega\setminus\Gamma_t}$ and (d) $t_2|_{\partial\Omega\setminus\Gamma_t}$, obtained using the fading regularization MFS algorithm, Morozov's discrepancy principle, $M_u = M_t = 40$, $N_{out} = 40$, $N_{int} = 20$, $d_1 = d_2 = 0.5$, $\lambda = 1.0 \times 10^{-2}$, $p_u \in \{1\%, 3\%, 5\% \}$ and $p_t = 0$, for the Cauchy problem (A) given by Example 1 with $\Gamma_u = \Gamma_t = \Gamma_{out}$, i.e. case (i).

retrieved using the fading regularization MFS algorithm, the stopping criterion (24b), $M_u = M_t = 40$, $N_{out} = 40$, $N_{int} = 20$, $d_1 = d_2 = 0.5$, $\lambda = 1.0 \times 10^{-2}$, and various amounts of noise added to the Dirichlet data on Γ_u , for the Cauchy problem (A) given by Example 1 with $\Gamma_u = \Gamma_t = \Gamma_{out}$. The corresponding exact and numerically reconstructed tractions $t_1|_{\partial\Omega\setminus\Gamma_t}$ and $t_2|_{\partial\Omega\setminus\Gamma_t}$ are displayed in Fig. 3(c) and (d), respectively. It can be seen from Fig. 3(a)–(d) that the fading regularization MFS algorithm presented in Sections 3 and 4 together with the discrepancy principle of Morozov (1966) produces very accurate and stable approximations for both the unknown displacement and traction vectors on Γ_{int} . Moreover, by increasing the numbers of collocation points and sources used in the MFS approximation, namely $M_u = M_t = 80$, $N_{out} = 80$, $N_{int} = 40$, and at the same time keeping unchanged the other parameters of the Cauchy problem (A) for Example 1 with $\Gamma_u = \Gamma_t = \Gamma_{out}$, i.e. $d_1 = d_2 = 0.5$, one obtains even more accurate numerical solutions for the displacement and the traction vectors on Γ_{int} , and these are presented in Fig. 4(a)–(d), respectively.

The fading regularization MFS algorithm, in conjunction with Morozov's discrepancy principle (24b), also produces very accurate and stable results with respect to decreasing the amount of noise in the data for the unknown boundary displacements and tractions on Γ_{out} the Cauchy problem (A) associated with the Example 1 with $\Gamma_u = \Gamma_t = \Gamma_{int}$, i.e. case (ii). These numerically reconstructed boundary data, together with their analytical counterparts, are displayed in Fig. 5(a)–(d), for $M_u = M_t = 40$, $N_{out} = 40$, $N_{int} = 20$, $d_1 = d_2 = 0.5$, $\lambda = 1.0 \times 10^{-2}$, $p_u \in \{1\%, 3\%, 5\% \}$ and $p_t = 0$.

The fading regularization MFS algorithm presented and analysed herein also produces very accurate, stable and convergent numerical results for a simply connected two-dimensional domain with a piecewise smooth geometry, such as the unit square centered in the

origin of the coordinate system considered in Example 2. Fig. 6(a)–(d) present the exact and numerical results for the unknown displacements, $u_1|_{\partial\Omega\setminus\Gamma_u}$ and $u_2|_{\partial\Omega\setminus\Gamma_u}$, and tractions, $t_1|_{\partial\Omega\setminus\Gamma_t}$ and $t_2|_{\partial\Omega\setminus\Gamma_t}$, respectively, retrieved using the fading regularization MFS algorithm, the stopping criterion (24b), $M_u = M_t = 60$, $N = 80$, $d = 2.0$, $\lambda = 1.0 \times 10^{-3}$, and various levels of noise added to $\mathbf{u}|_{\Gamma_u}$, for the Cauchy problem (A) given by Example 2, case (i). It can be seen that the numerical results obtained for both the unknown displacements and tractions on $\partial\Omega\setminus\Gamma_u$ and $\partial\Omega\setminus\Gamma_t$, respectively, are very good and stable approximations of their corresponding exact values.

The proposed fading regularizing MFS algorithm together with the stopping criterion (24b) works equally well for solving the inverse boundary value problem (B) for the Example 2, cases (ii) and (iii), as can be seen from Figs. 7 and 8, which present the numerically retrieved displacements on $\partial\Omega\setminus\Gamma_u$ and tractions on $\partial\Omega\setminus\Gamma_t$ in comparison with their corresponding analytical values. As can be noticed from these figures, again very accurate and stable reconstructions of the unknown Dirichlet and Neumann data are also obtained for the inverse boundary value problem (B) associated with the Example 2, cases (ii) and (iii).

In the case of Example 2, the relative RMS errors $e_{\partial\Omega\setminus\Gamma_u}(\mathbf{u})$ and $e_{\partial\Omega\setminus\Gamma_t}(\mathbf{t})$, retrieved using the fading regularization MFS algorithm described in Sections 3 and 4, the discrepancy principle (24b), $d = 2.0$, $p_u = 1\%$, $p_t = 0$ and an appropriate value for the parameter $\lambda > 0$, have the following values for the three inverse boundary value problems investigated:

- Case (i): $e_{\partial\Omega\setminus\Gamma_u}(\mathbf{u}) = 1.48 \times 10^{-3}$; $e_{\partial\Omega\setminus\Gamma_t}(\mathbf{t}) = 3.03 \times 10^{-3}$;
- Case (ii): $e_{\partial\Omega\setminus\Gamma_u}(\mathbf{u}) = 3.17 \times 10^{-3}$; $e_{\partial\Omega\setminus\Gamma_t}(\mathbf{t}) = 4.36 \times 10^{-3}$;
- Case (iii): $e_{\partial\Omega\setminus\Gamma_u}(\mathbf{u}) = 4.31 \times 10^{-3}$; $e_{\partial\Omega\setminus\Gamma_t}(\mathbf{t}) = 6.04 \times 10^{-3}$.

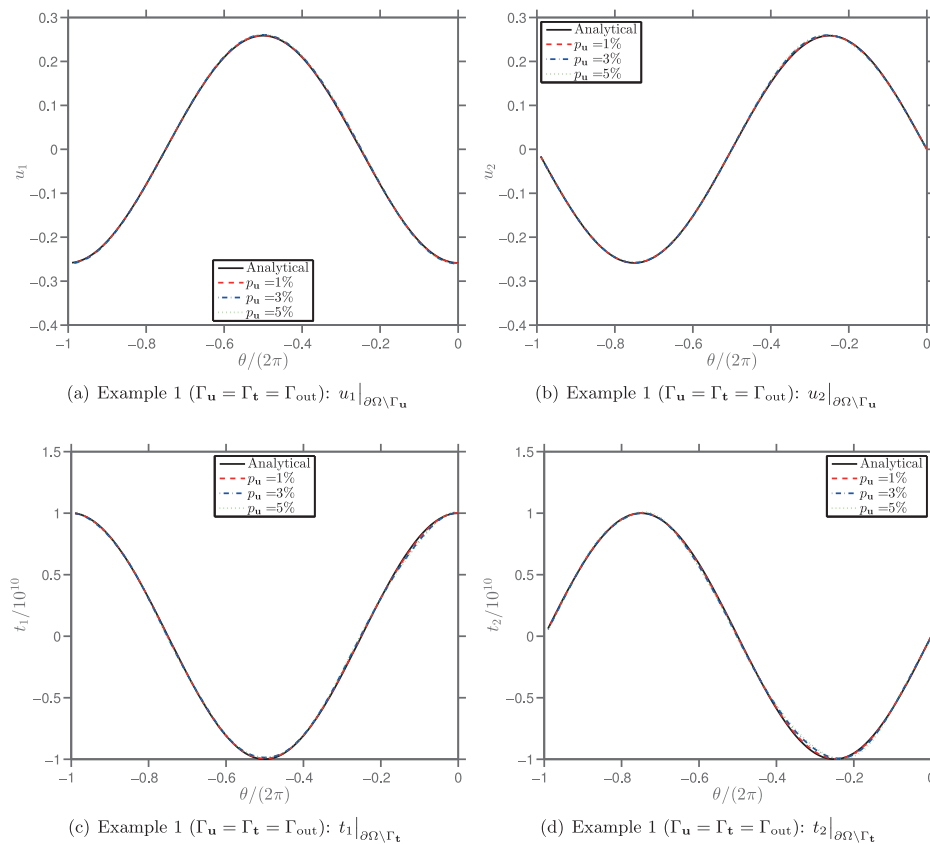


Fig. 4. The analytical and numerical displacements (a) $u_1|_{\partial\Omega\setminus\Gamma_u}$ and (b) $u_2|_{\partial\Omega\setminus\Gamma_u}$, and tractions (c) $t_1|_{\partial\Omega\setminus\Gamma_t}$ and (d) $t_2|_{\partial\Omega\setminus\Gamma_t}$, obtained using the fading regularization MFS algorithm, Morozov's discrepancy principle, $M_u = M_t = 80$, $N_{out} = 80$, $N_{int} = 40$, $d_1 = d_2 = 0.5$, $\lambda = 1.0 \times 10^{-2}$, $p_u \in \{1\%, 3\%, 5\% \}$ and $p_t = 0$, for the Cauchy problem (A) given by Example 1 with $\Gamma_u = \Gamma_t = \Gamma_{out}$, i.e. case (i).

It can be noticed that the values of both errors $e_{\partial\Omega\setminus\Gamma_u}(\mathbf{u})$ and $e_{\partial\Omega\setminus\Gamma_t}(\mathbf{t})$ increase with respect to the cases (i)–(iii) analysed herein. This is not surprising for the error $e_{\partial\Omega\setminus\Gamma_u}(\mathbf{u})$ since the length of the corresponding boundary on which the displacement vector \mathbf{u} is unknown and hence reconstructed numerically, i.e. $\Omega\setminus\Gamma_u$, increases with respect to the cases (i)–(iii), respectively. The fact that the same property also holds for the relative RMS error $e_{\partial\Omega\setminus\Gamma_t}(\mathbf{t})$ is a direct consequence of the length of the boundary on which over-specified data are prescribed, i.e. $\Gamma_u \cap \Gamma_t$, corresponding to the inverse boundary value problems associated with the cases (i)–(iii), respectively. More precisely, as expected, the more over-specified data is available for the inverse problem considered, the more accurate the missing boundary data reconstructed numerically, see also Figs. (6)–(8).

5.4. Sensitivity analysis

Next, we discuss the sensitivity of the numerical results obtained with respect to the distance from the sources to the boundary of the solution domain, as well as the parameter λ associated with the minimisation fading regularization functional (13), by considering, yet again, the Cauchy problem (A) for the Example 1, case (i). Table 1 presents the values of the relative RMS errors, $e_{\partial\Omega\setminus\Gamma_u}(\mathbf{u})$ and $e_{\partial\Omega\setminus\Gamma_t}(\mathbf{t})$, the convergence error (24a) and the number of iterations performed, k_{opt} , obtained when applying the fading regularization MFS algorithm with the stopping criterion (24b), $M_u = M_t = 40$, $N_{out} = 40$, $N_{int} = 20$, $d_1 = d_2 = 0.5$, perturbed Dirichlet data $\mathbf{u}|_{\Gamma_u}$ and various values of λ . The following conclusions can be drawn from Table 1:

- (a) For all levels of noise p_u and all values of λ considered, as expected, the inaccuracies in the numerical tractions are higher

Table 1

The values of the relative RMS errors, $e_{\partial\Omega\setminus\Gamma_u}(\mathbf{u})$ and $e_{\partial\Omega\setminus\Gamma_t}(\mathbf{t})$, the convergence error, E , and the corresponding number of iterations performed, k_{opt} , obtained using the fading regularization MFS algorithm, the stopping criterion (24b), $M_u = M_t = 40$, $N_{out} = 40$, $N_{int} = 20$, $d_1 = d_2 = 0.5$, $p_u \in \{1\%, 3\%, 5\% \}$, and various values of λ , for the Cauchy problem (A) given by Example 1, case (i).

λ	p_u	$e_{\partial\Omega\setminus\Gamma_u}(\mathbf{u})$	$e_{\partial\Omega\setminus\Gamma_t}(\mathbf{t})$	E	k_{opt}
5.0×10^{-1}	1%	1.08×10^{-2}	1.75×10^{-2}	1.32×10^{-2}	119
	3%	2.91×10^{-2}	5.08×10^{-2}	3.97×10^{-2}	91
	5%	4.70×10^{-2}	8.38×10^{-2}	6.62×10^{-2}	78
1.0×10^{-1}	1%	1.03×10^{-2}	2.29×10^{-2}	1.32×10^{-2}	27
	3%	2.76×10^{-2}	5.21×10^{-2}	3.82×10^{-2}	21
	5%	4.53×10^{-2}	8.11×10^{-2}	6.55×10^{-2}	18
5.0×10^{-2}	1%	1.03×10^{-2}	2.32×10^{-2}	1.29×10^{-2}	15
	3%	2.76×10^{-2}	5.16×10^{-2}	3.82×10^{-2}	12
	5%	4.68×10^{-2}	8.42×10^{-2}	6.55×10^{-2}	10
1.0×10^{-2}	1%	8.33×10^{-3}	2.18×10^{-2}	1.18×10^{-2}	6
	3%	2.23×10^{-2}	4.99×10^{-2}	3.55×10^{-2}	5
	5%	4.21×10^{-2}	8.22×10^{-2}	6.23×10^{-2}	4
5.0×10^{-3}	1%	1.01×10^{-2}	2.55×10^{-2}	1.25×10^{-2}	4
	3%	2.14×10^{-2}	5.65×10^{-2}	3.49×10^{-2}	4
	5%	4.38×10^{-2}	9.01×10^{-2}	6.27×10^{-2}	3
1.0×10^{-3}	1%	8.82×10^{-3}	3.78×10^{-2}	1.32×10^{-2}	3
	3%	2.37×10^{-2}	1.08×10^{-1}	3.97×10^{-2}	3
	5%	4.76×10^{-2}	1.27×10^{-1}	6.62×10^{-2}	2

than those in the numerical displacements since the former contain derivatives of the latter.

- (b) For each fixed value of λ , the relative RMS errors, $e_{\partial\Omega\setminus\Gamma_u}(\mathbf{u})$ and $e_{\partial\Omega\setminus\Gamma_t}(\mathbf{t})$, which measure the accuracy of the numerically reconstructed displacement and traction vectors, respectively,

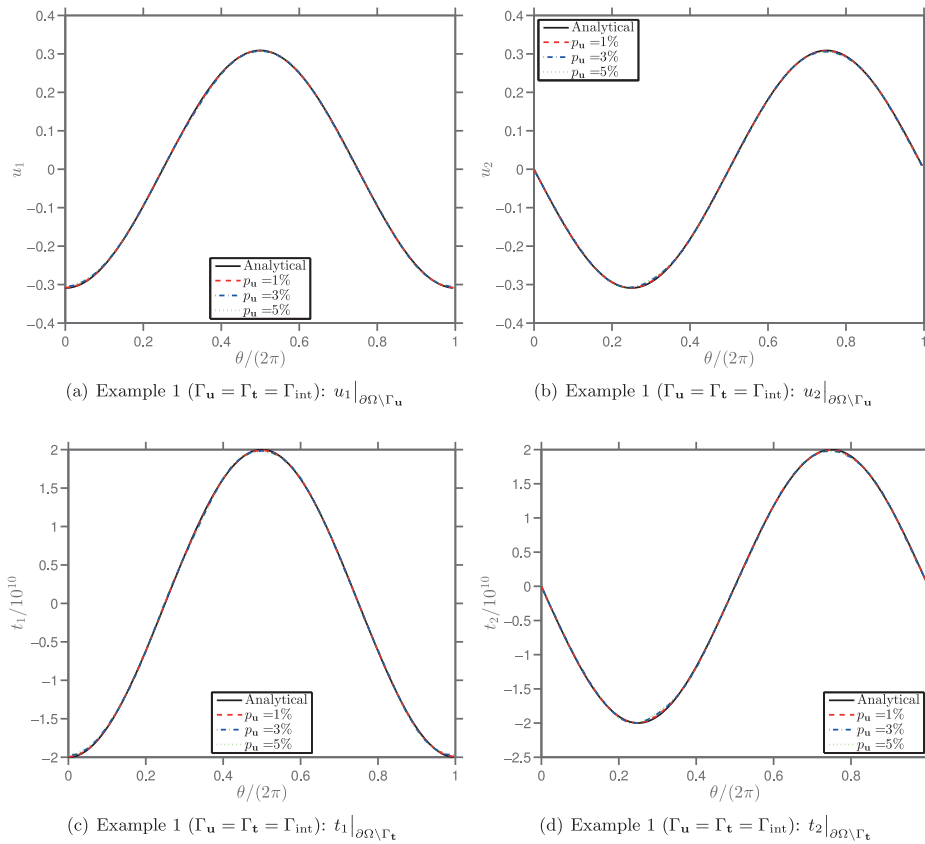


Fig. 5. The analytical and numerical displacements (a) $u_1|_{\partial\Omega\setminus\Gamma_u}$ and (b) $u_2|_{\partial\Omega\setminus\Gamma_u}$, and tractions (c) $t_1|_{\partial\Omega\setminus\Gamma_t}$ and (d) $t_2|_{\partial\Omega\setminus\Gamma_t}$, obtained using the fading regularization MFS algorithm, Morozov's discrepancy principle, $M_u = M_t = 40$, $N_{out} = 40$, $N_{int} = 20$, $d_1 = d_2 = 0.5$, $\lambda = 1.0 \times 10^{-2}$, $p_u \in \{1\%, 3\%, 5\%\}$ and $p_t = 0$, for the Cauchy problem (A) given by Example 1 with $\Gamma_u = \Gamma_t = \Gamma_{int}$, i.e. case (ii).

decrease with respect to decreasing the amount of noise added to the prescribed displacement vector $\mathbf{u}|_{\Gamma_u}$.

- (c) There is a relatively wide range of admissible values of λ to be used in the fading regularization functional (13), namely $\lambda \in [1.0 \times 10^{-3}, 5.0 \times 10^{-1}]$, for the inverse problem analysed in Table 1.
- (d) For each fixed amount of noise p_u and all admissible values of λ , the relative RMS errors, $e_{\partial\Omega\setminus\Gamma_u}(\mathbf{u})$ and $e_{\partial\Omega\setminus\Gamma_t}(\mathbf{t})$, are almost independent of λ , hence showing the robustness of the fading regularization algorithm with respect to the admissible value of λ chosen.
- (e) The number of iterations, k_{opt} , required for the fading regularization MFS algorithm to attain the convergence of the numerical solution according to Morozov's discrepancy principle (Morozov, 1966) decreases with respect to decreasing the parameter λ , with the mention that there is a certain range for the admissible values of the latter, see also (c).
- (f) The best numerical results, in terms of the accuracy, are obtained when the convergence error, E , has a value as close as possible to that of ε , i.e. the level of noise in the prescribed Cauchy data.

Similar conclusions can be drawn from Table 2, which tabulates the values of $e_{\partial\Omega\setminus\Gamma_u}(\mathbf{u})$, $e_{\partial\Omega\setminus\Gamma_t}(\mathbf{t})$, E and k_{opt} , obtained when applying the fading regularization MFS algorithm, the stopping criterion (24b), $M_u = M_t = 40$, $N_{out} = 40$, $N_{int} = 20$, $d_1 = 2.0$, $d_2 = 0.5$, $p_u \in \{1\%, 3\%, 5\%\}$ and various values of λ . By comparing Tables 1 and 2, it can be seen that, for the same number of MFS boundary collocation points, all levels of noise in the Dirichlet data $\mathbf{u}|_{\Gamma_{out}}$ and all admissible values of λ , the numerically retrieved solutions for the unknown displacements and tractions on Γ_{int} become more accurate

Table 2

The values of the relative RMS errors, $e_{\partial\Omega\setminus\Gamma_u}(\mathbf{u})$ and $e_{\partial\Omega\setminus\Gamma_t}(\mathbf{t})$, the convergence error, E , and the corresponding number of iterations performed, k_{opt} , obtained using the fading regularization MFS algorithm, the stopping criterion (24b), $M_u = M_t = 40$, $N_{out} = 40$, $N_{int} = 20$, $d_1 = 3.0$, $d_2 = 0.5$, $p_u \in \{1\%, 3\%, 5\%\}$, and various values of λ , for the Cauchy problem (A) given by Example 1, case (i).

λ	p_u	$e_{\partial\Omega\setminus\Gamma_u}(\mathbf{u})$	$e_{\partial\Omega\setminus\Gamma_t}(\mathbf{t})$	E	k_{opt}
5.0×10^{-1}	1%	9.50×10^{-3}	1.67×10^{-2}	1.32×10^{-2}	119
	3%	2.79×10^{-2}	4.74×10^{-2}	3.96×10^{-2}	91
	5%	4.58×10^{-2}	7.66×10^{-2}	6.59×10^{-2}	78
1.0×10^{-1}	1%	9.01×10^{-3}	1.62×10^{-2}	1.29×10^{-2}	27
	3%	2.64×10^{-2}	4.55×10^{-2}	3.87×10^{-2}	21
	5%	4.41×10^{-2}	7.44×10^{-2}	6.62×10^{-2}	18
5.0×10^{-2}	1%	9.14×10^{-3}	1.66×10^{-2}	1.29×10^{-2}	15
	3%	2.58×10^{-2}	4.51×10^{-2}	3.82×10^{-2}	12
	5%	4.56×10^{-2}	7.75×10^{-2}	6.56×10^{-2}	10
1.0×10^{-2}	1%	7.28×10^{-3}	1.69×10^{-2}	1.18×10^{-2}	6
	3%	2.12×10^{-2}	4.53×10^{-2}	3.55×10^{-2}	5
	5%	4.10×10^{-2}	7.64×10^{-2}	6.23×10^{-2}	4
5.0×10^{-3}	1%	8.93×10^{-3}	2.01×10^{-2}	1.25×10^{-2}	4
	3%	2.05×10^{-2}	5.29×10^{-2}	3.49×10^{-2}	4
	5%	4.27×10^{-2}	8.45×10^{-2}	6.27×10^{-2}	3
1.0×10^{-3}	1%	8.04×10^{-3}	3.54×10^{-2}	1.14×10^{-2}	3
	3%	2.31×10^{-2}	1.06×10^{-1}	3.40×10^{-2}	3
	5%	4.66×10^{-2}	1.23×10^{-1}	6.52×10^{-2}	2

when increasing the distance d_1 from the outer boundary Γ_{out} to its corresponding sources.

Finally, Table 3 presents the same values, namely $e_{\partial\Omega\setminus\Gamma_u}(\mathbf{u})$, $e_{\partial\Omega\setminus\Gamma_t}(\mathbf{t})$, E and k_{opt} , retrieved when applying the fading regularization MFS algorithm, the stopping criterion (24b), $M_u = M_t = 80$, $N_{out} = 80$, $N_{int} = 40$, $d_1 = d_2 = 0.5$, $p_u \in \{1\%, 3\%$,

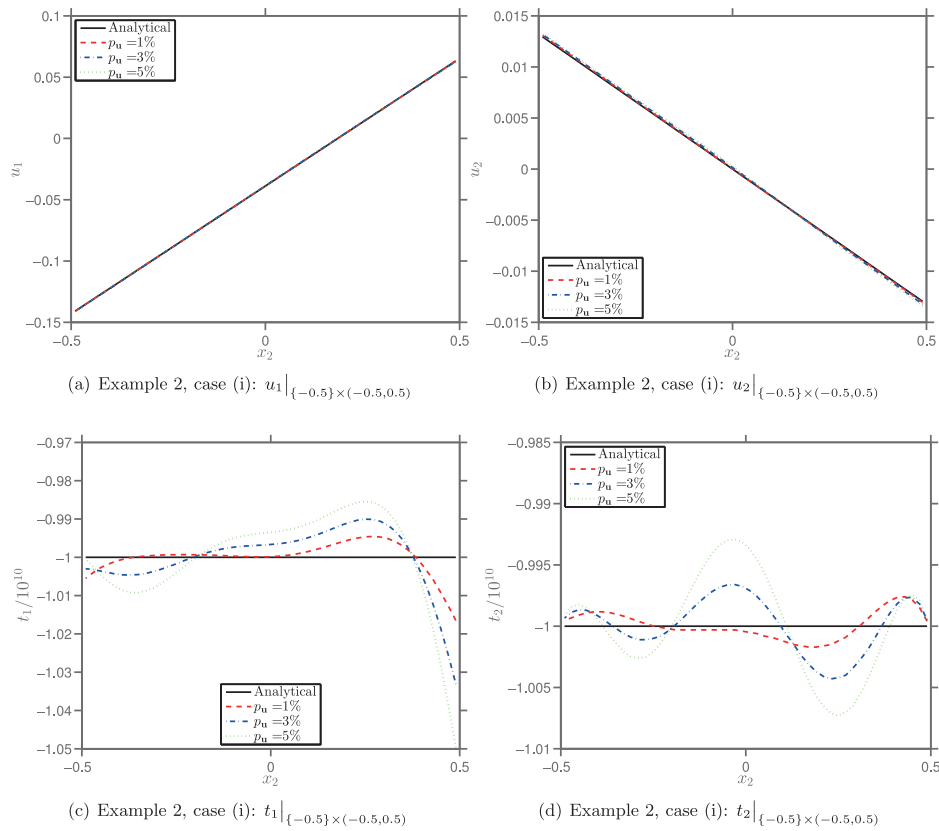


Fig. 6. The analytical and numerical displacements (a) $u_1|_{\{-0.5\} \times (-0.5, 0.5)}$ and (b) $u_2|_{\{-0.5\} \times (-0.5, 0.5)}$, and tractions (c) $t_1|_{\{-0.5\} \times (-0.5, 0.5)}$ and (d) $t_2|_{\{-0.5\} \times (-0.5, 0.5)}$, obtained using the fading regularization MFS algorithm, Morozov's discrepancy principle, $M_u = M_t = 60$, $N = 80$, $d = 2.0$, $\lambda = 1.0 \times 10^{-3}$, $p_u \in \{1\%, 3\%, 5\% \}$ and $p_t = 0$, for the Cauchy problem (A) given by Example 2, case (i).

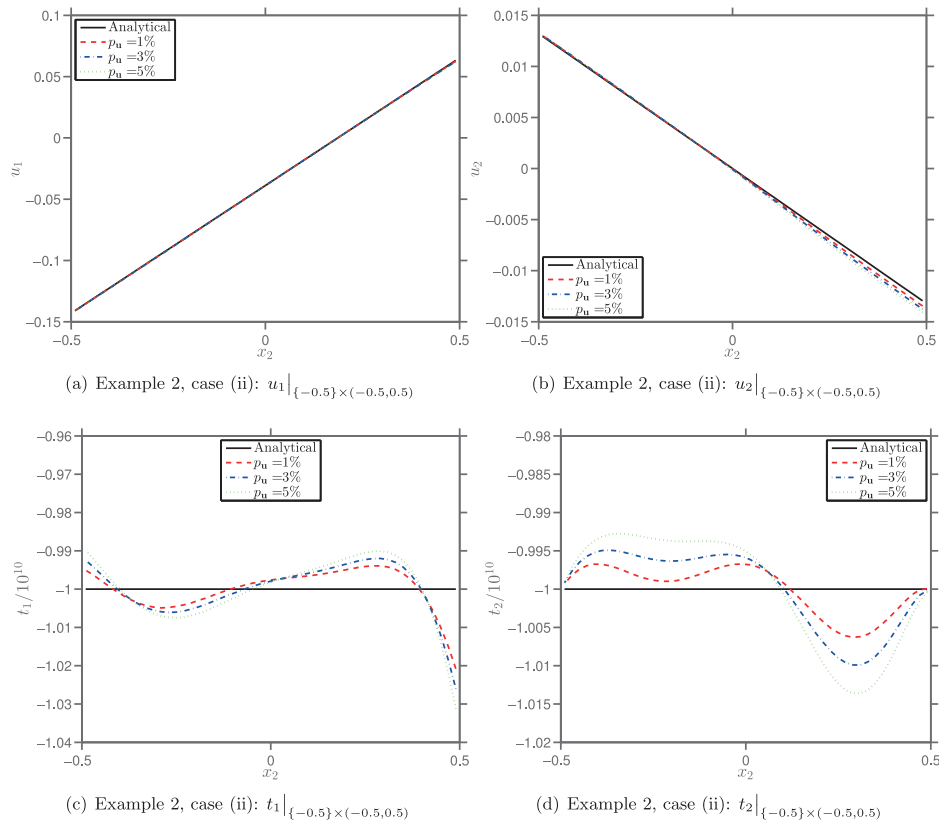


Fig. 7. The analytical and numerical displacements (a) $u_1|_{\{-0.5\} \times (-0.5, 0.5)}$ and (b) $u_2|_{\{-0.5\} \times (-0.5, 0.5)}$, and tractions (c) $t_1|_{\{-0.5\} \times (-0.5, 0.5)}$ and (d) $t_2|_{\{-0.5\} \times (-0.5, 0.5)}$, obtained using the fading regularization MFS algorithm, Morozov's discrepancy principle, $M_u = 40$, $M_t = 60$, $N = 80$, $d = 2.0$, $\lambda = 5.0 \times 10^{-4}$, $p_u \in \{1\%, 3\%, 5\% \}$ and $p_t = 0$, for the inverse boundary value problem (B) given by Example 2, case (ii).

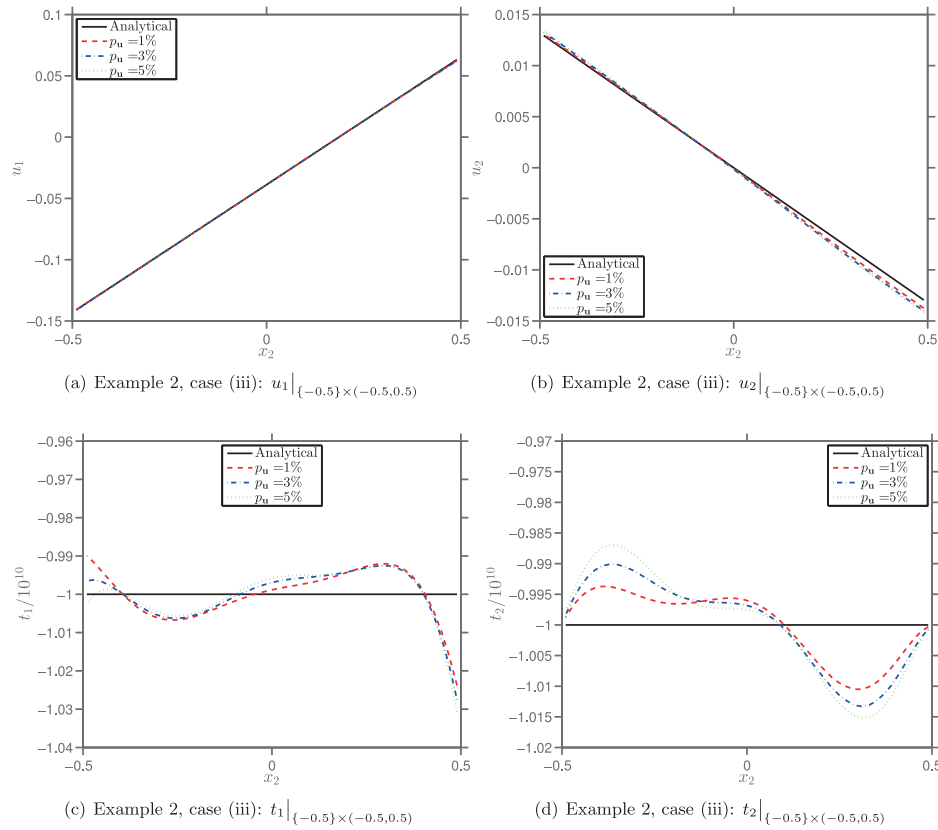


Fig. 8. The analytical and numerical displacements (a) $u_1|_{\{-0.5\} \times (-0.5, 0.5)}$ and (b) $u_2|_{\{-0.5\} \times (-0.5, 0.5)}$, and tractions (c) $t_1|_{\{-0.5\} \times (-0.5, 0.5)}$ and (d) $t_2|_{\{-0.5\} \times (-0.5, 0.5)}$, obtained using the fading regularization MFS algorithm, Morozov's discrepancy principle, $M_u = 20$, $M_t = 60$, $N = 80$, $d = 2.0$, $\lambda = 5.0 \times 10^{-3}$, $p_u \in \{1\%, 3\%, 5\% \}$ and $p_t = 0$, for the inverse boundary value problem (B) given by Example 2, case (iii).

Table 3

The values of the relative RMS errors, $e_{\partial\Omega \setminus \Gamma_u}(\mathbf{u})$ and $e_{\partial\Omega \setminus \Gamma_t}(\mathbf{t})$, the convergence error, E , and the corresponding number of iterations performed, k_{opt} , obtained using the fading regularization MFS algorithm, the stopping criterion (24b), $M_u = M_t = 80$, $N_{\text{out}} = 80$, $N_{\text{int}} = 40$, $d_1 = d_2 = 0.5$, $p_u \in \{1\%, 3\%, 5\% \}$, and various values of λ , for the Cauchy problem (A) given by Example 1, case (i).

λ	p_u	$e_{\partial\Omega \setminus \Gamma_u}(\mathbf{u})$	$e_{\partial\Omega \setminus \Gamma_t}(\mathbf{t})$	E	k_{opt}
5.0×10^{-1}	1%	3.38×10^{-3}	5.82×10^{-3}	1.52×10^{-2}	138
	3%	9.88×10^{-3}	1.61×10^{-2}	4.56×10^{-2}	110
	5%	1.63×10^{-2}	2.58×10^{-2}	7.60×10^{-2}	97
1.0×10^{-1}	1%	3.24×10^{-3}	5.72×10^{-3}	1.51×10^{-2}	31
	3%	9.45×10^{-3}	1.57×10^{-2}	4.52×10^{-2}	25
	5%	1.58×10^{-2}	2.54×10^{-2}	7.56×10^{-2}	22
5.0×10^{-2}	1%	3.38×10^{-3}	6.05×10^{-3}	1.52×10^{-2}	17
	3%	9.49×10^{-3}	1.61×10^{-2}	4.52×10^{-2}	14
	5%	1.46×10^{-2}	2.41×10^{-2}	7.47×10^{-2}	13
1.0×10^{-2}	1%	3.33×10^{-3}	6.73×10^{-3}	1.50×10^{-2}	6
	3%	9.67×10^{-3}	1.83×10^{-2}	4.50×10^{-2}	5
	5%	1.40×10^{-2}	2.73×10^{-2}	7.36×10^{-2}	5
5.0×10^{-3}	1%	3.00×10^{-3}	7.54×10^{-3}	1.46×10^{-2}	5
	3%	8.96×10^{-3}	1.98×10^{-2}	4.42×10^{-2}	4
	5%	1.42×10^{-2}	3.21×10^{-2}	7.30×10^{-2}	4
1.0×10^{-3}	1%	3.51×10^{-3}	1.21×10^{-2}	1.46×10^{-2}	3
	3%	1.03×10^{-2}	3.61×10^{-1}	4.33×10^{-2}	3
	5%	1.72×10^{-2}	6.02×10^{-1}	7.22×10^{-2}	3

5%} and various values of λ . By comparing Tables 1 and 3, we can conclude that for the same level of noise added to the data, distance from the sources to the boundary and value of λ , a refinement of the MFS discretisation provides us with more accurate numerical solutions for both $\mathbf{u}|_{\Gamma_{\text{int}}}$ and $\mathbf{t}|_{\Gamma_{\text{int}}}$, thus confirming, yet again, the convergence of the numerical solutions given by the fading

regularization MFS algorithm with respect to increasing the number of MFS boundary collocation points.

6. Conclusions

In this paper, we have studied the numerical reconstruction of the missing displacements and tractions on an inaccessible part of the boundary for two-dimensional linear isotropic elastic materials from over-prescribed noisy measurements taken on the remaining accessible boundary part. Two types of inverse problems, given by Eqs. (1), (6a), (6b) and (7), were solved by combining the fading regularization method presented in Section 3 with the MFS described in Section 4. The iterative procedure was stopped according to the discrepancy principle of Morozov (1966). Five inverse problems for a simply connected domain with a piecewise smooth boundary and a doubly connected domain with a smooth boundary, respectively, have been thoroughly investigated concerning the accuracy, convergence, stability and sensitivity of the numerical solution with respect to the problem parameters of the numerical results.

From the numerical results obtained and presented in Section 5, we can conclude that the fading regularization MFS algorithm described, analysed and implemented in this paper provides us with very accurate, convergent and stable numerical results for boundary data reconstruction problems in two-dimensional isotropic linear elasticity, for a wide range of values of the admissible parameter λ , at the same time being a very robust and versatile iterative algorithm for inverse boundary value problems in elasticity. Future extensions of the fading regularization MFS algorithm are currently under investigation and they refer to inverse boundary value problems associated with two-dimensional isotropic and anisotropic heat

conduction, Helmholtz-type equations and linear thermoelasticity, as well as the corresponding three-dimensional inverse problems.

Acknowledgments

Liviu Marin acknowledges the financial support received from the Romanian National Authority for Scientific Research (CNCS–UEFISCDI), project number PN–II–ID–PCE–2011–3–0521. A part of this research was carried out whilst the first author was visiting the University of Caen–Lower Normandy.

References

- Andrieux, S., Baranger, T.N., 2008. An energy error-based method for the resolution of the Cauchy problem in 3D linear elasticity. *Comput. Methods Appl. Mech. Eng.* 197, 902–920.
- Bonnet, M., Constantinescu, A., 2005. Inverse problems in elasticity. *Inverse Probl.* 21, R1–R50.
- Cimetière, A., Delvare, F., Jaoua, M., Pons, F., 2001. Solution of the Cauchy problem using iterated Tikhonov regularization. *Inverse Probl.* 17, 553–570.
- Cimetière, A., Delvare, F., Jaoua, M., Pons, F., 2002. An inversion method for harmonic functions reconstruction. *Int. J. Therm. Sci.* 41, 509–516.
- Cimetière, A., Delvare, F., Pons, F., 2000. Une méthode inverse à régularisation évanescence. *Comptes Rendus de l'Académie des Sciences – Série IIb – Mécanique* 328, 639–644.
- Comino, L., Marin, L., Gallego, R., 2007. An alternating iterative algorithm for the Cauchy problem in anisotropic elasticity. *Eng. Anal. Bound. Elem.* 31, 667–682.
- Delvare, F., Cimetière, Pons, F., 2002. An iterative boundary element method for Cauchy inverse problems. *Comput. Mech.* 28, 291–302.
- Delvare, F., Cimetière, A., Hanus, J.L., Bailly, P., 2010. An iterative method for the Cauchy problem in linear elasticity with fading regularization effect. *Comput. Methods Appl. Mech. Eng.* 199 (49–52), 3336–3344.
- Delvare, F., Hanus, J.L., 17–20 May 2005. Complément de données par méthode inverse en élasticité linéaire. In: 7eme Colloque National en Calcul de Structures. Giens, France.
- Ellabib, A., Nachaoui, A., 2008. An iterative approach to the solution of an inverse problem in linear elasticity. *Math. Comput. Simul.* 77, 189–201.
- Fairweather, G., Karageorghis, A., 1998. The method of fundamental solutions for elliptic boundary value problems. *Adv. Comput. Math.* 9, 69–95.
- Gao, Z., Mura, T., 1991. Elasticity problems with partially overspecified boundary conditions. *Int. J. Eng. Sci.* 29, 685–692.
- Golberg, M.A., Chen, C.S., 1999. The method of fundamental solutions for potential, Helmholtz and diffusion problems. In: Golberg, M.A. (Ed.), *Boundary Integral Methods: Numerical and Mathematical Aspects*, Computational Engineering, vol. 1. WIT Press/Computational Mechanics Publications, Boston, MA, pp. 103–176.
- Golub, G.H., Heath, M., Wahba, G., 1979. Generalized cross-validation as a method for choosing a good ridge parameter. *Technometrics* 22, 1–35.
- Gorzelańczyk, P., Kołodziej, J.A., 2008. Some remarks concerning the shape of the shape contour with application of the method of fundamental solutions to elastic torsion of prismatic rods. *Eng. Anal. Bound. Elem.* 32, 64–75.
- Hadamard, J., 1923. *Lectures on Cauchy's Problem in Linear Partial Differential Equations*. Yale University Press, New Haven.
- Hansen, P.C., 1998. Rank-Deficient and Discrete Ill-Posed Problems: Numerical Aspects of Linear Inversion. SIAM, Philadelphia.
- Huang, C.H., Shih, W.Y., 1997. A boundary element based solution of an inverse elasticity problem by conjugate gradient and regularization method. In: *Proceedings of the 7th International Offshore Polar Engineering Conference*. Honolulu, USA, pp. 338–395.
- Karageorghis, A., Lesnic, D., Marin, L., 2011. A survey of applications of the MFS to inverse problems. *Inverse Probl. Sci. Eng.* 19, 309–336.
- Koya, T., Yeh, W.C., Mura, T., 1993. An inverse problem in elasticity with partially overspecified boundary conditions. II. Numerical details. *Trans. ASME J. Appl. Mech.* 60, 601–606.
- Kozlov, V.A., Maz'ya, V.G., Fomin, A.V., 1991. An iterative method for solving the Cauchy problem for elliptic equations. *Zhurnal Vychislitel'noi Matematiki i Matematicheskoi Fiziki* 31, 64–74. English translation: U.S.S.R. Computational Mathematics and Mathematical Physics 31, 45–52, 1991.
- Kupradze, V.D., Aleksidze, M.A., 1964. The method of functional equations for the approximate solution of certain boundary value problems. *Comput. Math. Math. Phys.* 4, 82–126.
- Liu, Q.G., Šarler, B., 2014. Non-singular method of fundamental solutions for anisotropic elasticity. *Eng. Anal. Bound. Elem.* 45, 65–78.
- Marin, L., 2005. A meshless method for solving the Cauchy problem in three-dimensional elastostatics. *Comput. Math. Appl.* 50, 73–92.
- Marin, L., 2009. The minimal error method for the Cauchy problem in linear elasticity. Numerical implementation for two-dimensional homogeneous isotropic linear elasticity. *Int. J. Solids Struct.* 46, 957–974.
- Marin, L., Elliott, L., Ingham, D.B., Lesnic, D., 2001. Boundary element method for the Cauchy problem in linear elasticity. *Eng. Anal. Bound. Elem.* 25, 783–793.
- Marin, L., Elliott, L., Ingham, D.B., Lesnic, D., 2002a. Boundary element regularization methods for solving the Cauchy problem in linear elasticity. *Inverse Probl. Eng.* 10, 335–357.
- Marin, L., Hao, D.N., Lesnic, D., 2002b. Conjugate gradient-boundary element method for the Cauchy problem in elasticity. *Q. J. Mech. Appl. Math.* 55, 227–247.
- Marin, L., Johansson, B.T., 2010a. A relaxation method of an alternating iterative algorithm for the Cauchy problem in linear isotropic elasticity. *Comput. Methods Appl. Mech. Eng.* 199, 3179–3196.
- Marin, L., Johansson, B.T., 2010b. Relaxation procedures for an iterative MFS algorithm for the stable reconstruction of elastic fields from Cauchy data in two-dimensional isotropic linear elasticity. *Int. J. Solids Struct.* 47, 3462–3479.
- Marin, L., Lesnic, D., 2002a. Regularized boundary element solution for an inverse boundary value problem in linear elasticity. *Commun. Numer. Methods Eng.* 18, 817–825.
- Marin, L., Lesnic, D., 2002b. Boundary element solution for the Cauchy problem in linear elasticity using singular value decomposition. *Comput. Methods Appl. Mech. Eng.* 191, 3257–3270.
- Marin, L., Lesnic, D., 2004. The method of fundamental solutions for the Cauchy problem in two-dimensional linear elasticity. *Int. J. Solids Struct.* 41, 3425–3438.
- Marin, L., Lesnic, D., 2005. Boundary element–Landweber method for the Cauchy problem in linear elasticity. *IMA J. Appl. Math.* 18, 817–825.
- Martin, T.J., Haldermann, J.D., Dulikravich, G.S., 1995. An inverse method for finding unknown surface tractions and deformations in elastostatics. *Comput. Struct.* 56, 825–835.
- Mathon, R., Johnston, R.L., 1977. The approximate solution of elliptic boundary value problems by fundamental solutions. *SIAM J. Numer. Anal.* 14, 638–650.
- Morozov, V.A., 1966. On the solution of functional equations by the method of regularization. *Soviet Math. Doklady* 7, 414–417.
- Schnur, D., Zabarav, N., 1990. Finite element solution of two-dimensional elastic problems using spatial smoothing. *Int. J. Numer. Methods Eng.* 30, 57–75.
- Tikhonov, A.N., Arsenin, V.Y., 1986. *Methods for Solving Ill-Posed Problems*. Nauka, Moscow.
- Turco, E., 1999. A boundary elements approach to identify static boundary conditions in elastic solids from stresses at internal points. *Inverse Probl. Eng.* 7, 309–333.
- Yeh, W.C., Koya, T., Mura, T., 1993. An inverse problem in elasticity with partially overspecified boundary conditions. I. Theoretical approach. *Trans. ASME J. Appl. Mech.* 60, 595–600.